WIRELESS COMMUNICATIONS AND MOBILE COMPUTING
Wirel. Commun. Mob. Comput. 2016; **16**:1837–1850
Published online 9 December 2015 in Wiley Online Library (wileyonlinelibrary.com). DOI: 10.1002/wcm.2653

RESEARCH ARTICLE

Three dimensional compressed sensing for wireless networks-based multiple node localization in multi-floor buildings

Mohamed Amine Abid and Soumaya Cherkaoui*

Electrical and Computer Engineering, University of Sherbrooke, Sherbrooke, Canada

ABSTRACT

In wireless network-based node localization, the received signals are hampered by complex phenomena, such as shadowing, noise, and multi-path fading. In this work, the localization is stated as an ill-posed problem that can be solved by compressed sensing (CS) technique. A three dimensional (3D)-CS approach using the ratio of received signal strength (R2S2) and the time difference of arrival metrics was proposed to improve the localization accuracy of multiple target nodes in 3D wireless networks, and to reduce deployment complexity and processing time. Simulation and experimental tests were conducted in a large multi-floors building using the strength of the received signals and the radio map of the localization area. The results indicated that the 3D-CS approach is reliable for identifying the floor number and estimating the horizontal position. The localization precision is less affected by the propagation medium variation than the conventional 2D-CS method. The localization mean error is lower when the number of access points increases, and the radio map spacing decreases. In addition, the accuracy of the 3D-CS approach was assured as well as the building material characteristics, position of access points, and wireless-terminal real transmission power are unknown. Copyright © 2015 John Wiley & Sons, Ltd.

KEYWORDS

compressed sensing; localization in 3D WNs; indoor positioning; RTLS

***Correspondence**

Soumaya Cherkaoui, Electrical and Computer Engineering, University of Sherbrooke, Sherbrooke, Canada.
E-mail: soumaya.cherkaoui@usherbrooke.ca

1. INTRODUCTION

The Global Positioning System (GPS) [1] is the widely adopted navigation system for tracking and navigation assistance applications. In outdoor environments, the GPS determinates the longitude of a receiver position with acceptable accuracy. The altitude estimation is up to three times less accurate than longitude even with high-quality GPS receivers. This work focuses on accurate 3D localization in indoor and dense urban environments with limited GPS satellites visibility [2,3]. Indoor localization is an important and challenging issue. In fact, recent studies show that people spend up to 90% of their lifetime indoor and 54% of world population lives in urban areas [4].

Many Real Time Localization Systems (RTLS) [5] have been proposed for indoor localization in wireless networks (WNs) in the last two decades. Geometric, probabilistic, and ray-tracing (RT) techniques based on empirical/theoretical electromagnetic wave propagation models are often used for node position estimation. The lack of reliability of localization techniques based on WNs is due to several factors; WN infrastructures that support the localization are not designed for this task, the propagation medium variation, and the multi-path propagation in non-line of sight (NLOS) condition. To achieve better accuracy, recent RTLS use additional equipment (accelerometers, cameras, laser, or sonar sensors) that increase the deployment cost and difficulty for large-scale location based service applications. In addition, the most existing RTLS differentiate between horizontal and elevation localization accuracy and focus more on the former.

Compressed sensing (CS) [6,7] is an emerging technology promising for a wide range of applications especially in signal and image processing. This work proposes a new localization method based on CS approach, which can recover target positions with accuracy from few noisy measurements in 3D WNs.

The proposed method is appropriate for indoor and outdoor environments when the positions of access points (APs), the equivalent isotropic radiated power (EIRP) of

wireless transmitters, and the environment characteristics (layout, materials, etc.) are unknown. In the offline phase, the radio map of the detection area is created by taken received signal measurements at multiple reference points (RPs). In the online phase, multiple node positions estimation is performed based on the real-time measurements from of APs. In order to reduce the localization mean error due to the propagation medium variation, it is recommended to use dual metrics, that is, the ratio of received signal strength (R2S2) [8] instead of the received signal strength (RSS), and respectively the time difference of arrival (TDOA) instead of the time of arrival (TOA). The use of R2S2 and TDOA metrics requires processing a radio map and measurement data set represented by n-way arrays leads to 3D-CS issue. The 3D-CS method using the R2S2 metric aims to provide a reliable localization with low sensitivity to noisy measurements, acceptable running time, and without additional equipment. The method estimates at once the horizontal positions and the elevation of target nodes with the same precision.

The paper is organized as follows: firstly, a survey of related works on localization in 3D WNs and a background on CS theory were presented. Secondly, a multiple node localization problem was formulated as a recovery problem, and the resolution process that uses CS theory with different signal metrics was described in detail. Thirdly, the performance of the proposed method was investigated by conducting simulation and experimental tests in a multi-floor building (MFB) with existing WN infrastructure. The impact of different parameters such as the propagation medium variation, the number of APs, and RP on localization mean error was investigated. Finally, the performance of the 3D-CS method was compared with the 2D-CS methods and others, exiting RTLS.

2. RELATED WORKS ON WIRELESS NETWORKS-BASED LOCALIZATION IN MULTI-FLOOR BUILDING

Localization techniques in WNs can be classified in four groups: proximity methods, geometric methods, scene analyses, and RT. Proximity methods determine whether the target is within the read range of an AP with known position. This allows coarse localization related to the APs density and coverage depending on the wireless technology. For fine-grained localization, geometric methods are used in two forms: (i) triangulation method estimates the target position by calculating the distance to at least three APs with known positions. The distance that separates the target and the AP is computed from RSS attenuation and radio wave propagation models, or from the TOA of the signal traveling at the speed of the light; and (ii) angulation method estimates the target position from the intersection of angle direction lines from at least two APs. Scene analyses methods, such as the fingerprinting localization, are composed of two phases. In the offline phase, the fingerprints (TOA, RSS, and direction of arrival (DOA)) of signal received are recorded at multiple reference points (RPs) through the localization area and stored in a reference data set (radio map). In online phase, the position of target node is estimated by matching its real-time fingerprints with those in the radio map. The matching of fingerprints can be performed with a multitude of techniques such as least-square minimization, Kalman filtering, and Bayesian approaches [9,10]. The RT technique is able to simulate a wide variety of optical effects, such as reflection, scattering, and dispersion phenomena. Thus, the RT was perceived as a promising solution for indoor localization in WNs with NLOS condition. Alas, RT is heavy in vector analysis, which involves high computational cost of the system.

People and assets localization in MFB and 3D areas is an important and challenging problem [11]. Given the increasing trend of tall buildings construction in most cities of the world, indoor vertical localization becomes as important as horizontal. In many works addressing the floor estimation, the horizontal localization within the floor is not considered or deteriorated. Several studies have addressed horizontal and vertical localization issue in MFB. Varshavsky *et al.* [12] developed the fingerprinting-based localization system using GSM technology. SkyLoc system aims to locate the actual floor of a mobile user who dials 911 in tall MFB. Experimentations were conducted in six MFBs with 9–16 floors in three cities across North America. Using RSS, SkyLoc system succeeds to identify the correct floor, one floor-off, and two floors-off in 57%, 82%, and 98% of the cases, respectively. Ahmed *et al.* [13] explored the idea of locating targets in a semantically meaningful area (SMA) in MFB instead of using geometric distance. Using IEEE 802.11 beacons, the exact SMA and floor of the target node were determined in 83% and 88% of cases, respectively. The localization system based on radio interferometry achieved an accuracy of few centimeters in an area of 160-m range by making measurements with at least eight network nodes [14]. Such system takes about 1 min to estimate the position of the target, and it is appropriate for stationary target localization, because a mobile target, such a pedestrian, can cross several tens of meters in 1 min.

In robotic research, a high precision is required. For example, the precision of several tens of centimeters requires micro aerial vehicles to navigate autonomously in a MFB using onboard sensors [15]. Schwarz *et al.* [16] have proposed an Ultra Wide Band-based 3D positioning system that performed a localization mean error of 0.5 m in a room of $9.6 \times 8 \times 2.8$ m size. Simultaneous localization and mapping (SLAM) [17] allows an autonomous robot to build the map of an environment and simultaneously locate its position. Woodman and Harle [18] developed a pedestrian tracking system in a three-floor building using a foot-mounted inertial sensor to track the sensor-wearer with an accuracy of 1 m. Hightower *et al.* [19] developed SpotOn localization system using long-range RFID tags coupled with two-axis accelerometer with an accuracy of 1 m^3 in ideal conditions. Additional

equipment, such as gyroscope or accelerometer, improves the localization precision, but it is not appropriate for largely deployed applications.

In RT research field, the work reported in [20] achieved a mean localization error of 10 m in an urban area of 120 m side length in NLOS condition with the presence of obstacles. Tayebi *et al.* [21] used RT and fingerprinting techniques and obtained a best mean error of 0.55 m in a detection area of 85 × 120 m size with an RPs spacing of 0.8 m and an eight-ray-order of path. RT-based techniques improve the localization precision in NLOS condition, when geometric methods may probably return erroneous results, but they are time consuming.

Compressed sensing approach was recently applied for network monitoring, sparse events detection, distributed sensing, and lately for localization in WNs. Results reported in [22] indicated good localization performance when locating 15 target nodes based on 90 measurements in an area of 60 × 60 m divided into a 900 grids with a signal noise ratio (SNR) of 25 dB. More recently, simulation results achieved in [23] proved the accuracy of an adaptive localization algorithm based on distributed CS in wireless sensor networks. The positions of 10 target nodes are exactly estimated (with a near zero error) in a 20×20 m size network divided into a 500 grids when SNR is 20 dB, and some 150 sensor nodes are randomly deployed in the area. CS was also used to build the map of obstacles in the environment based on sparse sensing [24].

In this work, a new 3D-CS approach is proposed for localization in MFB with NLOS condition based on signal metrics with no additional equipment. The proposed technique allows the same double accuracy for vertical and horizontal position estimation with an acceptable running time.

3. RELATED WORKS ON COMPRESSED SENSING

Compressed sensing technique has recently emerged in applied mathematics and has been widely used for signal and image processing. CS allows signal acquisition and lossless data compression using reduced sampling rate far less than Nyquist–Shannon rate (twice the higher frequency of signal). Indeed, high sampling rate requires considerable number of sensors and associated acquisition lines, and it generates large amount of data to be processed. To obviate these limitations, CS theory proposes to compress sparse signals at the sampling phase with particular method, that is, directly on sensors level.

Compressed sensing exploits the sparse nature of signals and allows their reconstruction with a high probability from small number of samples by solving a convex optimization problem. Let us consider a discrete field or signal x represented by a column vector of dimension N. Assume that x has a sparse representation in a given basis Ψ composed of N rows vector $\{\Psi_i\}$, when $1 \leq i \leq N$. The signal x is written as

$$x = \sum_{i=1}^{N} \theta_i \Psi_i \tag{1}$$

where the vector θ of dimension N represents the coefficients of x in basis Ψ. Signal x is said k-sparse when k among N coefficients in $\theta_i$are non-zero. CS is useful when the signal has parsimonious representation in the basis Ψ, that is, $K \ll N$, so that CS promises to reconstruct a signal x from M random measurements where $M \geq (K \log(N/K))$ and $M \ll N$ [7]. Instead of measuring θ directly respecting to Shannon's rate, the CS method modifies the framework for data acquisition and presumes taking compressed measurements as presented in the following model:

$$y = \Phi x = \Phi \Psi \theta = \Phi^* \theta \tag{2}$$

where Φ is the $M \times N$ transformation matrix, and the $M \times 1$ column vector measurements $\hat{y}$ is the linear projections of x onto Φ. Thus, y is presented as an ill-posed problem. Recovering the signal x from the observation measurement y is equivalent to resolve a system of highly under determined linear equations. However, in CS theory, the sparse vector x can be recovered in polynomial time under some assumptions. Mainly, the transformation matrix Φ^* must conserve the restricted isometric property between y and signal x to be reconstructed later. This property is satisfied with high probability if the matrix Φ and Ψ are incoherent. The inconsistency is made, for example, if Φ is a random matrix.

The problem presented in (2) admits an infinite number of approximate solutions $\tilde{x}$. Because the evaluation of the norm l_0 is a non-convex problem difficult to solve, the norm l_1 minimization resulting in a convex problem as presented in (3) is applied. This problem can be efficiently solved by using existing algorithms such the basis pursuit (BP) algorithm [25].

$$\min \|\tilde{x}\|_1 \text{ such that } \Phi \tilde{x} = y \tag{3}$$

In the case of noisy measurements, a zero-mean error parameter (err) is added to (2) as follows:

$$y = \Phi \tilde{x} + eps = \Phi^* \theta + err \tag{4}$$

Thus, x can be recovered by using greedy algorithms, such as Matching Pursuit [26] or BP Denoising (BPDN) [27], which are defined to resolve optimization problem in the following form:

$$\min \|\tilde{x}\|_1 \text{ such that } \|\Phi \tilde{x} - y\|_2 < eps \tag{5}$$

where $\|err\|_2$ is lower than eps.

The topic of 3D-CS usefulness for 3D applications was primarily addressed in image processing field. In recent works, 3D-CS was applied for 3D shape reconstruction and tracking assets location in 3D space using magnetic resonance imaging (MRI) and ultrasonic imaging technologies.

The feasibility and challenges of 3D-CS use in MRI applications was investigated in [28]. Quinsac *et al.* [29] have defined a CS-based solution for the reconstruction of a 3D scene by transmitting wideband ultrasonic pulses and analyzing their reflections received by an array of sensors.

Feng *et al.* [30,31] were the first to propose RTLS using CS theory in WNs. CS was used to estimate single and multiple target positions with acceptable accuracy in a 2D indoor environment from a small number of RSS measurements. The authors have exploited the spatial sparse nature of localization in WNs problem, to, firstly, formulate it as a sparse vector recovery problem in discrete spatial domain, and secondly to recover target node positions by solving a l_1-minimization problem. A localization error of 0.4 m was observed in simulation when four target nodes are located in a 10×10 m area divided on 23×23 grids using 12 RSS measurements and assuming a SNR equal to 25 dB [30].

In the next section, we will present how to use the RSS (respectively TOA) and the R2S2 (respectively TDOA) metrics for localization in MFB based on CS. The localization in WNs problem formulation and the multi-linear algebra process applied with full 3D-CS approach will be exposed.

4. 3D-CS-BASED LOCALIZATION IN MFB

Time of arrival and RSS metrics are the most used measurements in WNs-based RTLS. The time-based method measures the time delay of signal from the transmitter to receiver to deduce the distance that separates them. The TDOA metric is aimed to improve location accuracy in NLOS condition when a high-resolution clock and inter-node synchronization are in place. Regarding RSS metric, the distance is proportional to the attenuation suffered by the signal to attain the receiver. The inconvenience of the use of RSS is due to the propagation medium variation and multi-path propagation. In addition, the theoretical or empirical radio propagation models allow an approximation of the distance between the transmitter and receiver. The R2S2 metric is intended to alleviate position estimation errors intrinsic to the RSS measurements.

The proposed 3D-CS method uses a fingerprinting localization technique based on R2S2 or TDOA metric, and a 3D-CS approach for the fingerprints matching and position estimation of multiple wireless nodes. It should be noted that the proposed method has the same form with TOA and RSS, and a different form in greater dimension with TDOA and R2S2 metrics. In the first form, RSS or TOA is measured between the target node and one AP (single metric). The resultant radio map and measurement data are presented by 2D matrix. In the second form, TDOA or R2S2 metric concerns the target node and two APs simultaneously (dual metric). The radio map and measurement data set are presented by three-way arrays, and a 3D-CS procedure is used for localization in WNs.

Compressed sensing is thrifty in terms of sensing resources, which can be helpful where they are not available at large number. In localization in WNs case, the APs are installed to optimally cover specifics areas in the MFB, and they are not planned for localization purpose. CS is perfectly suited to recover target positions from small number of measurements to quickly estimate the position and improve the system responsiveness. It is important to emphasize that in this context is not a question of signals recovery, so that no matter of conventional signal time variation problem. The interest is to detect the target nodes presence, pinging on the network at a discrete time t with, to measure the RSS level, and to estimate their positions.

4.1. Problem formulation

The following sub-sections provide a formal expression of the proposed method for localization in 3D WNs using single and dual metrics.

4.1.1. 2D-CS-based position recovery program with single metrics (RSS and TOA).

The MFB is decomposed in a set of superposed grids. Each RP position is represented by its index in a vector. For example, if each floor is decomposed on 10×10 grids, the four-floor building requires a vector of size 400 to represent all RPs index. Assume that RP_i with index $i = 128$, so it located in the grid of coordinates $(3, 8)$ in the second floor. The radio map in represented by the following matrix:

$$\Psi_{K\times N} = \begin{pmatrix} \psi_{1,1} & \cdots & \psi_{1,N} \\ \vdots & \ddots & \vdots \\ \psi_{K,1} & \cdots & \psi_{K,N} \end{pmatrix} \tag{6}$$

where $\psi_{i,j}$ is the RSS measured at RP_j from AP_i, for $i = 1, 2, \ldots, K$ and $j = 1, 2, \ldots, N$, and K and N are the total number of APs and RPs, respectively.

During online phase, only a sub-set of APs existing in target nodes read range is considered. Additional selection criteria of APs can be used based on signal strength or covariance. The first criterion discards the APs with RSS value lower to a specific threshold and the second selects the APs with minimum RSS readings variance. The measurement matrix $\Phi_{L\times K}$ represents the indexes of L selected APs for the current localization cycle. Each Φ_l row vector in the measurement matrix means that $\mathrm{AP_l}$ is located at the $\mathrm{index_i}$ in the established APs indexes order $\Phi_l = [\Phi_1, \ldots, \Phi_{k-1}, 1, \Phi_{k+1}, \ldots, \Phi_K]$.

At a given time, every target node has a unique position in the discrete spatial domain. All target nodes present in the localization area at an instant t are represented by the sparse matrix $\theta_{N\times T}$, where T is the total number of existing targets and each column vector θ_k has whose cells equal to zero expect this corresponding to the position of target node, $\theta_k = [\theta_1, \ldots, \theta_{n-1}, 1, \theta_{n+1}, \ldots, \theta_N]^T$. Taking our previous example, if the filed at index $\theta_{128} = 1$ in the recovered vector θ_l^*, the target node is located at the position of coordinates (3, 8) in the second floor.

Finally, the compressed RSS measurements that are recorded by all target nodes from selected APs are represented by the $L \times T$ matrix $y = \Phi\Psi\theta + \varepsilon$ where ε is a random measurement noise and the matrix θ is the solution to be found.

To be able to properly apply CS, two essential conditions must be fulfilled, namely, the θ parsimony, already proved, and the incoherence of Φ and Ψ [9]. However, the reference matrix Ψ and measurement matrix Φ are artlessly coherent in spatial domain. Thus, an orthogonalization procedure is applied in order to introduce the incoherence condition. Assume that $y' = Ty$ and $T = ZA^{\dagger}$, where $A = \Phi\Psi$ and $Z = \text{orth}\left(A^T\right)^T$. Note that orth (.), $(.)^T$ and $(.)^{\dagger}$ are the orthogonal basis, the transpose and the pseudo-inverse of matrix, respectively. This procedure transforms the matrix Z in orthogonal. The new compressed measurements are then presented as follows:

$$y' = ZA^{\dagger}y_m = ZA^{\dagger}A\,\theta + ZA^{\dagger}\varepsilon = Z\,\theta + \varepsilon' \quad (7)$$

This problem formulation was already proposed by Feng *et al.* [30,31] to localize multiple target nodes in 2D WN using RSS metric.

4.1.2. 3D-CS position recovery program with dual metrics (R2S2 and TDOA).

As mentioned earlier, with R2S2 and TDOA metrics, we have to handle n-way arrays because each reading entry is computed according to a pair-wise of APs and one wireless node. Then a 3-way array structure, called tensor, is employed to represent the radio map Ψ as follows:

$$\Psi_{K\times K\times N} = \begin{pmatrix} \psi_{1,1,1} & \cdots & \psi_{1,K,N} \\ \vdots & \ddots & \vdots \\ \psi_{K,1,1} & \cdots & \psi_{K,K,N} \end{pmatrix} \quad (8)$$

The radio map is a tensor in mode-1 of column vector $\psi_{i,j,n}$, where $i = 1, 2, \ldots K, j = 1, 2, \ldots K$, and $n = 1, 2, \ldots, N$ with K and N are the total number of APs and RPs, respectively. Using R2S2 metric, $\psi_{i,j,n}$ is the ratio of RSS reading from AP_i to that from AP_j ratio at RP_n position. With TDOA metric, $\psi_{i,j,n}$ is the difference of arrival time of signal transmitted from AP_i minus that from AP_j recorded at RP_n position.

The matrix of targets positions $\theta_{N\times T}$ and the measurement matrix $\Phi_{L\times K}$ working are identical to the previous section. The online compressed measurement tensor $y_{L\times L\times T}$ records values (R2S2 or TDOA) calculated from all selected APs pair-wises in targets read range in the localization area as follows:

$$y = \Psi\times_{2|3}\Phi\times_1\theta + \varepsilon \quad (9)$$

where ε is the measurement noise ant operator $\times_{2|3}$ means that the tensor the Ψ is successively multiplied in mode-2 ($\times_2$) and in mode-3 ($\times_3$) by the matrix Φ. The resulted tensor is multiplied in mode-1 ($\times_1$) by the matrix of target positions θ. In order to effectively recover θ via l_1-minimization algorithm by CS theory, Ψ and Φ must be incoherent. The following transformation aims to orthogonalize the n-way arrays, so the matrix Φ will have dense representation in the basis Ψ.

First, assume that

$$y' = T\times_n y, \text{ with } T = Z\times_n A^{\dagger} \text{ and } Z = \text{HOSVD}(A^T)^T \quad (10)$$

where $A = \Psi\times_{2|3}\Phi$ and Z is the transpose of high-order singular value decomposition (HOSVD) [32] of A^T. Notice that the transpose of tensor A is made by permuting his two modes 1 and 2, which amount to transpose all horizontal slices of tensor [33]. The HOSVD model allows the tensor $\mathcal{T}$ decomposition into one core entity $\mathcal{G}$ and three matrices factors as follows;

$$\mathcal{T} = [\![\mathcal{G}; A, B, C]\!] \approx \mathcal{G}\times_1 A\times_2 B\times_3 C \quad (11)$$

where matrices factors $(A; B; C)$ are generally orthogonal, and the core tensor $\mathcal{G}$ has mutually orthogonal slices in the three modes of $\mathcal{T}$ as illustrated in Figure 1.

Combining equations (9) and (10), we obtain

$$\begin{aligned} y' = Z\times_n A^{\dagger}\times_n y &= Z\times_n A^{\dagger}\times_n A\times_1\theta + Z\times_n A^{\dagger}\times_n\varepsilon \\ &= Z\times_1\theta + Z\times_n A^{\dagger}\times\varepsilon \end{aligned}$$

$$y' = Z\times_1\theta + \varepsilon' \quad (12)$$

The model in (12) can be applied because $A^{\dagger}\times_n A = I_n$ where I_n is the mode-n identity tensor and $\times_n$ is the mode-n product with n = 3 (three modes of tensor).

Once all conditions are met, namely, the sparsity of θ, the orthogonality of Z and the incoherence of Ψ and Φ, it is possible to recover the multiple target locations matrix approximation θ^* in accordance with CS theory by solving a l_1-minimization problem. Finally, the tensors Z and y' are reshaped as matrices, and the optimization solver algorithms are applied as the same way as in 2D problem. In noiseless case, the well-known BP algorithm is selected to solve the problem modeled as follows:

$$\theta^* = \min_\theta \|\theta\|_1 \text{ s.t.} Z\times_1\theta = y'. \quad (13)$$

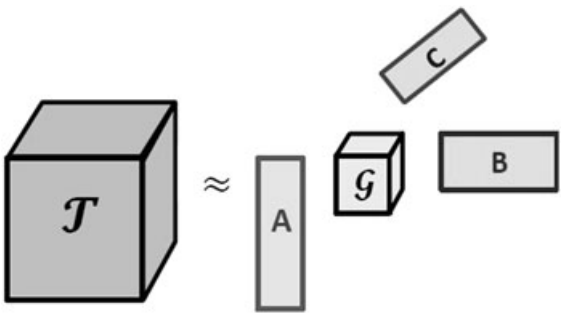

Figure 1. Tucker decomposition.

The BP algorithm is used to solve an optimization problem using noisy data, as indicated in [25]. To evaluate the performance of the proposed method versus various noises level, BPDN algorithm is applied to solve the following problem:

$$\theta^* = \min_\theta \|\theta\|_1 \text{ s.t. } \left\|Z \times_1 \theta - y'\right\|_2 < \varepsilon' \quad (14)$$

The target positions are recovered from the $N \times T$ matrix θ^*, and each $N \times 1$ column vector represents the position of one target. If this vector contains few non-zero coefficients among all N, the greatest coefficient is selected, otherwise the centroid of positions with highest coefficients is computed to estimate the final position as given later:

$$Q^* = \text{Centroid}\left((x_t, y_t, z_t) \,|\theta^*(t) \geq \max(\theta^*(t)) \times 0.95\right) \quad (15)$$

5. SIMULATIONS RESULTS

In this work, we focus on evaluating the performances of the proposed method with RSS and R2S2 metrics in both simulation and experimentation. Experime ntation with TOA and TDOA metrics will be the focus of future work.

Two scenarios were studied. In the first scenario, LOS propagation condition is considered in order to evaluate the performance of the proposed localization method in ideal conditions. In the second scenario, NLOS condition is considered using a reproduction that is close to the real MFB where the experiments were performed to simulate WN conditions as in reality. To enable better comparison, the dimensions of localization areas are identical in both scenarios. The radio map created in offline phase aggregates all RSS values computed according to the selected radio propagation model. The RSS from all APs are computed at every discrete RP location in detection area without considering noises. To create the radio map tensor based on R2S2 metric, the same measurements are used to calculate the ratio of RSS values with reference to all pairs of APs at every discrete RP. The average of 100 target localization operations was performed for each study presented in sections 5 and 6.

5.1. Localization in MFB with LOS condition

The objective of this study is to validate the efficiency of the proposed method and to analyze the influence of propagation medium variation on localization accuracy in LOS condition. The free space-shadowing model is used to simulate the ideal case with LOS propagation. The lognormal shadowing model [34] is applied to deal with dynamic changes in propagation medium by introducing a random noise to the measurements. The path loss in terms of distance obeys to the following power law:

$$PL(d)\,[dBm] = PL_{d_0} + 10n\,log\left(\frac{d}{d_0}\right) + X_\sigma \quad (16)$$

where PL_{d_0} represents the attenuation at a reference distance d_0, n is the path loss exponent that defines the rate at which RSS decreases with distance in a specific environment, d is the distance between transmitter and receiver, and X_σ is a Gaussian random variable of received power (in dBm) with zero mean and a standard deviation σ. With a confidence level C, the normality range of $X_\sigma \in [z\sigma \text{ dBm}, +z\sigma \text{ dBm}]$ and $z = {Q_x}^{-1}\left(\frac{c+1}{2}\right)$. The value of Z can be obtained from a Normal distribution table.

Simulation setup: Localization area considered in LOS condition is reduced to an open space without indoor walls or roofs equivalent to 4 floors with superficies of 80×60 m each. A total of 30 APs are simulated to create the radio map with $40 \times 30 \times 4$ RPs, so that the horizontal distance between two neighbors RPs is equal to 2 m, and it is fixed to 4 m in vertical direction. Wi-Fi APs illustrated by circles annotated with the floor number are dispersed throughout the MFB as seen in Figure 2. A battery of tests was conducted to localize four targets at unknown positions supposed at RPs locations. When all the APs are used, the minimum number of measurements required by CS theory is respected ($30 > 4 \times log(40 \times 30 \times 4/4)$).

Simulation Evaluation: The purpose of this first simulation is to evaluate the impact of the propagation medium variation on the 3D-CS method performance. In the first case, there is no change considered in propagation medium during online localization phase. The real-time RSS measurements are strictly equal to those recorded in radio map ($X_\sigma = 0$). In this situation, the localization program based on RSS as well as with R2S2 succeeds at every run to recover accurately the target positions, as visualized in Figure 2. Indeed, the problem is reduced to an inverse problem where the radio map defines the model that relates each vector of RSS measurements to a specific position in the MFB.

In the second case, a random noise is added to the real-time measurements by setting the maximum standard deviation (σ) to 2, 5, 10, and 15 dBm, which corresponds to different levels of propagation medium variation. Figure 3 summarizes the localization mean error and the corresponding standard deviation (represented by error bars) obtained with respect to different propagation variation levels. Using RSS and 2D-CS approach, the obtained mean error in horizontal position is equal to 2.15 m with a standard deviation of 1.44 m when $\sigma = 10$ dBm. The current target floor is always well recovered with a lower variation. However, one floor is missed in 38% of cases when $\sigma = 10$ dBm.

In presence of radio propagation irregularity, a new hypothesis is considered using R2S2 metric. Assuming a homogeneous environment at one slot time, the signal strength variation between the target and each of the two considered AP has the same sign, which makes R2S2

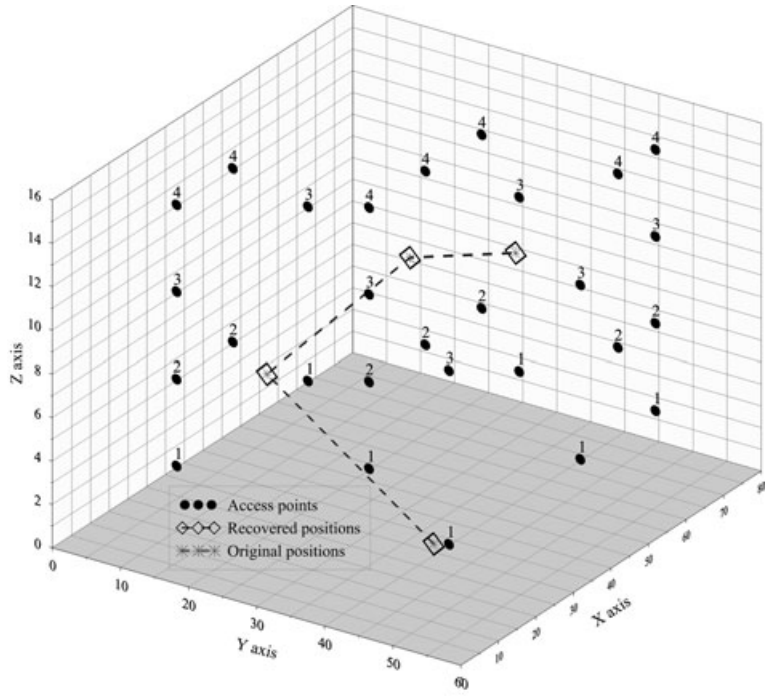

Figure 2. Recovered target positions using 3D-CS method in ideal conditions.

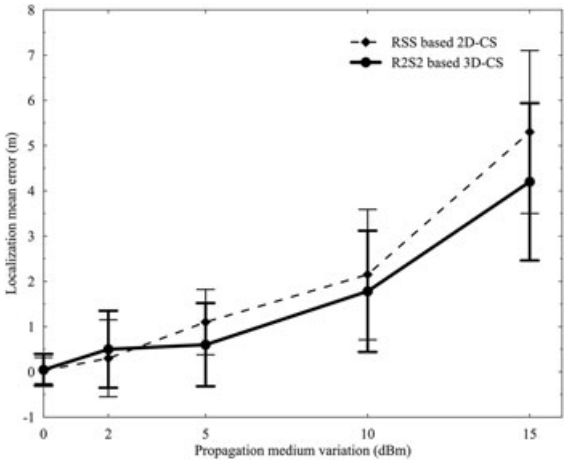

Figure 3. Influence of the propagation medium variation on the localization mean error for 2D-CS and 3D-CS methods.

metric less sensitive to the propagation medium variations. In other terms, the ratio of RSS from a pair of APs varies little with environment change as the RSS from either Wi-Fi APs often increases or decreases simultaneously. Simulations results demonstrate that localization accuracy is notably improved, mainly when $\sigma \geq 10$ dBm as shown in Figure 3. For example, the horizontal mean error is equal to 1.78 m with a standard deviation of 1.35 m when $\sigma = 10$ dBm. The right floor can be well determined even with noisy measurements.

As seen in Figure 3, with both methods based on RSS and R2S2 metrics, the localization error increases as the propagation variation increases and the accuracy decreases sharply when the variation is close to 15 dBm. The error standard deviation is relative stable when σ is set to 2 and 5 dBm, and it increases gradually when $\sigma \geq 10$ dBm. The 3D-CS method allows superior performance to recover target positions with lower localization mean error and corresponding standard deviation compared with the 2D-CS method, especially with high propagation variation. It should be noted that the position recovery process is not reliable when $\sigma \geq 15$ dBm.

Figure 4 shows the percentage of the exact position, the neighbor, and the centroid which correspond to the lower, middle, and upper portion of the histogram, respectively. The exact position is often recovered with higher percentage using the both methods and whatever the value of σ. Otherwise, one neighbor position or the centroid of a given number of likely positions is selected as the estimated target position.

5.2. Localization in MFB with NLOS condition

Several empirical and theoretical models [34] have been proposed in literature to correlate signals path loss with respect to the distance between a transmitter and a receiver in indoor buildings with obstacles. In this work, the multi-walls multi-floors model [35] is selected for simulations in NLOS condition. This model, derived from the ray tracing algorithm, considers the number and the type of walls and

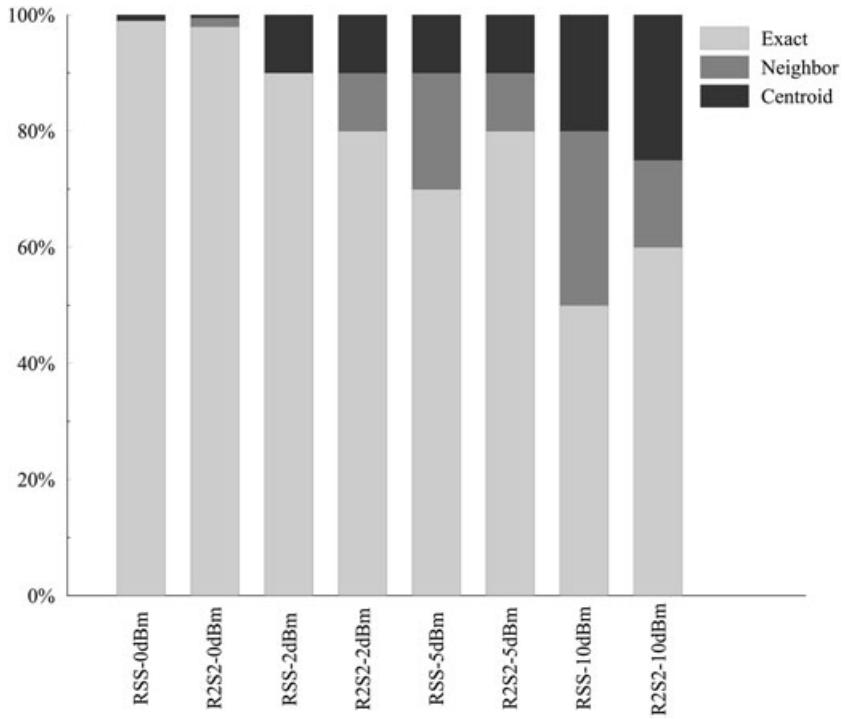

Figure 4. Details of recovered positions using RSS and R2S2 metrics with different propagation medium variation levels in LOS condition.

floors as detailed in the following formula:

$$PL = PL_{d_0} + 10n \log\left(\frac{d}{d_0}\right) + \sum_{i=1}^{I} \sum_{k=1}^{K_{wi}} L_{wik} + \sum_{j=1}^{J} \sum_{k=1}^{K_{fj}} L_{fjk} \quad (17)$$

where L_{wik} denotes the attenuation due to k-th traversed wall of type i, $L_{fjk}$is the attenuation due to k-th traversed floor of type j, i and j are the wall and floor types respectively, K_{wi} is the number of traversed walls of category i, K_{fj} is the number of traversed roofs of category j and finally PL is the estimated path loss. Notice that when no walls and floors are present between the transmitter and the receiver, the model is artlessly shortened to the free space propagation model presented in (16).

Simulation setup: The MFB structure selected in this study reflects the most real propagation conditions in common interior trim of hospitals, airports, commercial center, and so on. The real-like plan of environment chosen for experimentation was implemented. The MFB is considered as an inseparable entity insuring that the accuracy of the localization in vertical direction is as important as in horizontal direction. The floors and the walls are represented by plans and polygons, respectively, as seen in Figure 5. The intersection of wave trajectory with the walls and the floors was computed exactly by algebraic equations. Because the walls and the ceilings are made with different materials and having different thickness, through-wall and through-floor power attenuation are set to 5 and 15 dBm, respectively. These values are based on work in [35] that experimentally measured the path loss depending on the material and thickness of obstacles in MFB using 2.4-GHz wireless technologies. The placement of the APs is picked as it is in the real MFB in order to reduce their number while providing good wireless network coverage. The inter-floor signal propagation makes the radio map more cohesive and very advantageous for localization issue. Even though the received signals are weak (not useful to establish communication), they still supply additional and pertinent information for localization purpose. In NLOS condition, performed tests consist on locating simultaneously four target nodes on exact RP positions. The 3D-CS method was compared with the 2D-CS method using different simulation parameters.

Simulation results: Figure 6 summarizes the localization mean error determined with different levels of propagation medium variation (0, 2, 5, 10, and 15 dBm) and by varying the number of the APs of 10, 20, and 30. The selected APs are equivalent to the number of measurements in CS theory having a minimum required of 12.32, considering $(40 \times 30 \times 4)$ RPs and four target nodes. Similarly to LOS condition, the results showed that localization mean error increases as the propagation medium variation increases using 2D-CS and 3D-CS methods. The 3D-CS method tolerates higher level of propagation medium variation up to 15 dBm using 20 and 30 APs. The localization mean error significantly decreases as the number of APs

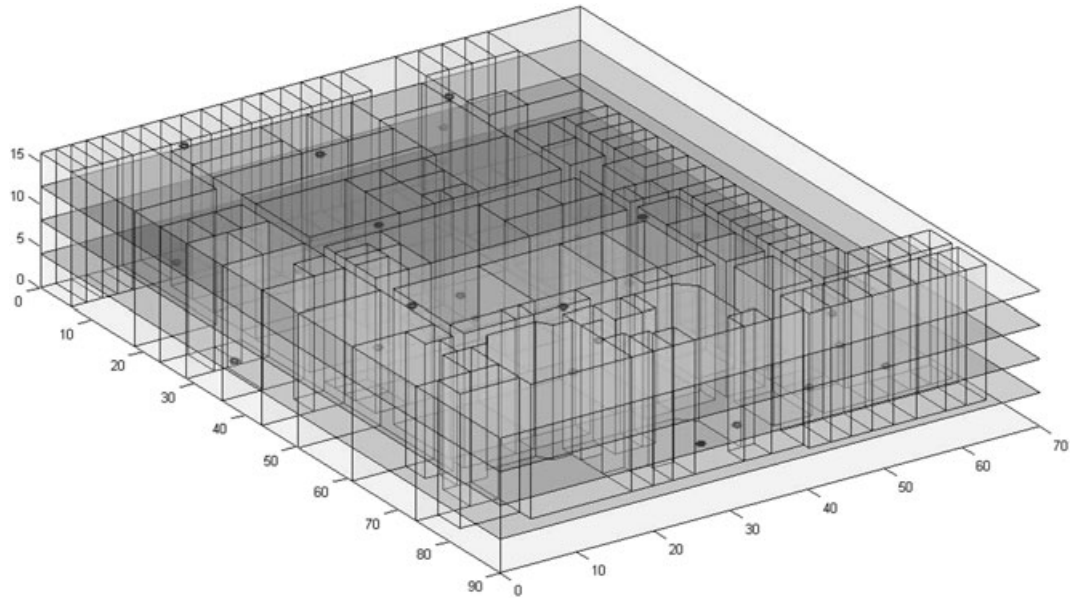

Figure 5. Reproduction of the MFB plan.

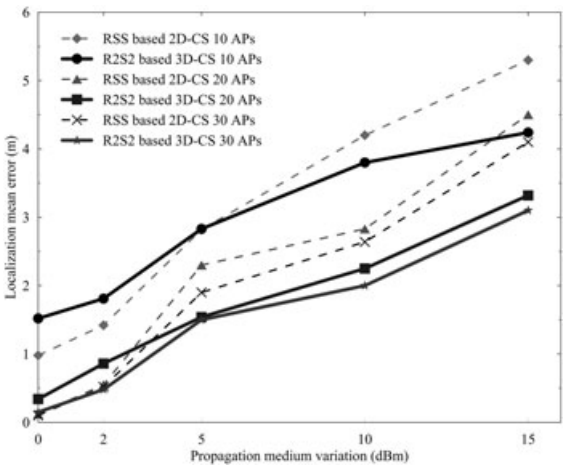

Figure 6. The localization mean error determined by varying the propagation medium variation and the number of APs using 2D-CS and 3D-CS methods in NLOS condition.

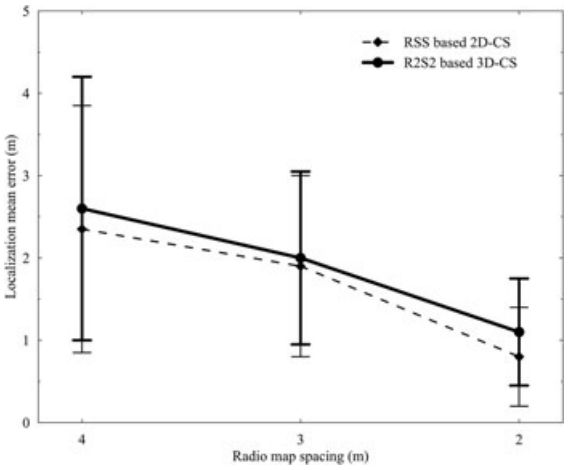

Figure 7. Influence of the radio map spacing on localization mean error.

increases from 10 to 20 exceeding the minimum required by CS theory.

In order to analyze the impact of radio map spacing on the localization mean error, both 2D-CS and 3D-CS localization methods were simulated under various levels of horizontal distance (2, 3, and 4 m) between two adjacent RPs. In this scenario, unknown target node positions were located somewhere in the vicinity of RPs using 30 APs with no propagation medium variation. As shown in Figure 7, the closer the radio map spacing results in a decrease of the localization mean error and the standard deviation.

Based on the previous simulation results, the average of the localization mean error is equal to 1.97 and 2.19 m with an average of the standard deviation of 1.22 and 1.62 m using the 3D-CS and the 2D-CS method, respectively. As a result, the 3D-CS method is found to be suitable for localization in MFB in NLOS condition. Thus, the semantically meaningful area can be well identified. The disparities of RSS measurements between adjacent positions, which are often separated by walls or ceilings, in complex MFB structures are clearer than those observed in open-space area.

6. EXPERIMENTAL RESULTS

Experiments were carried out to assess the performance of the proposed localization method in a real MFB. The accuracy of the 3D-CS localization method was investigated by varying the number of APs, the radio map spacing, and the number of target nodes. The performance of the proposed method was compared with 2D-CS and other conventional methods addressing the same problem in similar conditions.

Experimental setup: The experiments were conducted in the four-floor building of the faculty of engineering at the University de Sherbrooke. Each floor measures 80 m in length, 60 m in width, and 4 m in height and comprises around 100 premises. Unlike residential or commercial buildings, the materials and the equipment of the selected MFB are different from one floor to another and even from one compartment to another. In this spirit, the experimental site was fittingly selected in order to experiment different materials and building structures. The real plan of the third floor of the building is shown in Figure 8. Seven or eight APs were installed in each floor, as illustrated by circles annotated by letters from A to G, for a total of 30 APs in the entire MFB. Note that the AP locations are different from one floor to another.

To create the radio map, the RSS values were measured from APs in the read range of the Wi-Fi scanner at 128 RPs through corridors of each floor and exactly in front of each door. Each two adjacent RPs are separated by 2 m at 1.5 m above the floor. A minimum of 6 APs and a maximum of 14 APs were detected at each RP. To prevent any interference with the RSS measurements, the radio map was created during the non-activity period of the building. At each RP, the Wi-Fi scanner program was run over a sufficiently period (at least 30 s) until the RSS measurements are stabilized and all APs are detected. The total run time to investigate all the floors was about 12 h. Finally, the RSS scanning files were analyzed to create the radio map data

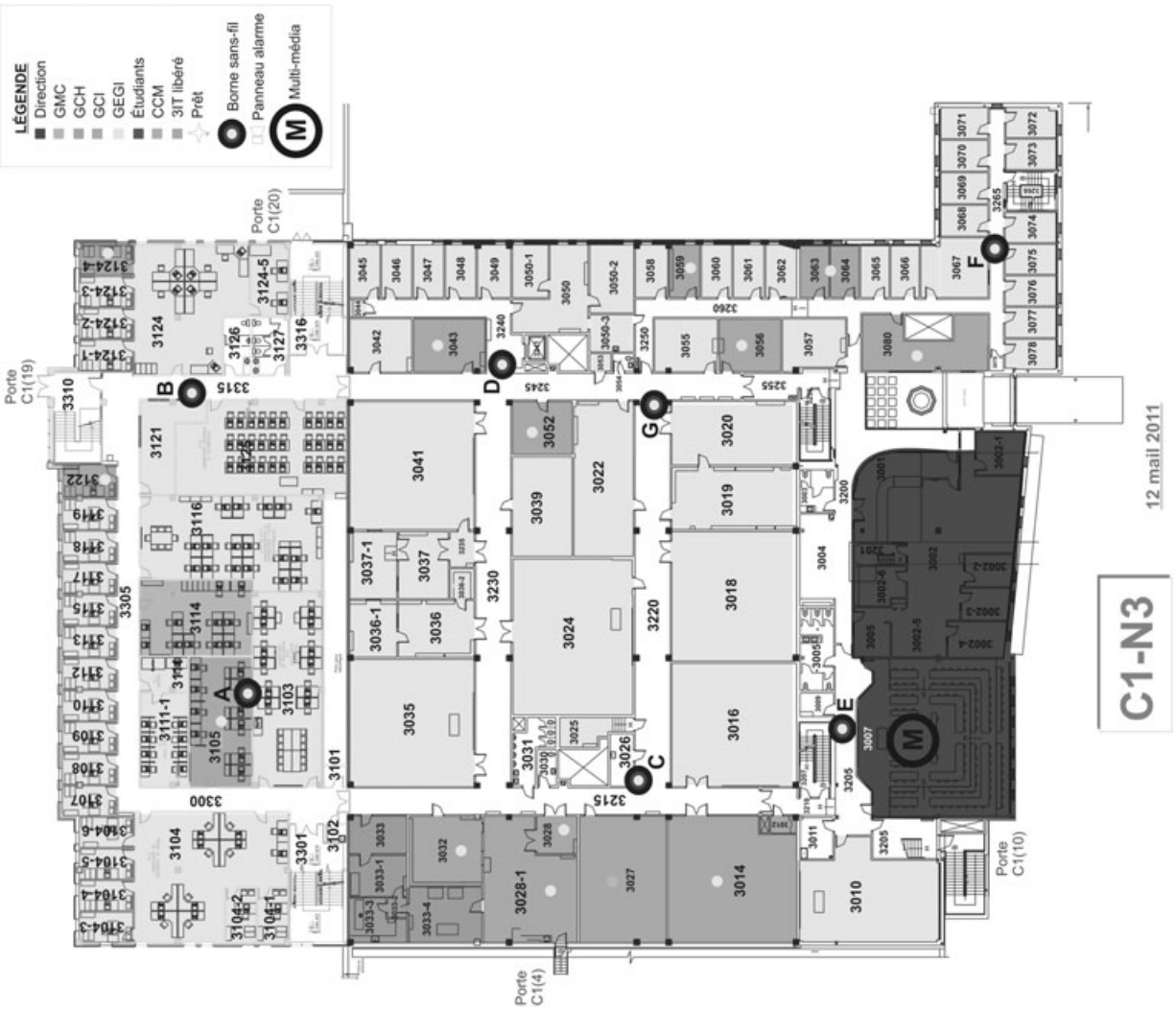

Figure 8. Plan of the third floor of MFB and APs placement.

Wirel. Commun. Mob. Comput. 2016; **16**:1837–1850 © 2015 John Wiley & Sons, Ltd.
DOI: 10.1002/wcm

set and to dress the correspondence table between the RP positions and their corresponding semantically meaningful area. An Intel Core 2 quad with 4GB memory computer was used to perform all the calculations. The radio map for the 2D-CS is presented by an array of 30×512 that records the RSS values from the 30 APs at the 512 RP positions. Note that the minimum number of measurements required by CS theory is 8.42 when using 512 RPs and 4 target nodes. For the 3D-CS method, the radio map consists of a tensor of $30 \times 30 \times 512$ that calculates the RSS of AP_i to the RSS of AP_j ratio at a RP_k, where i and j vary between 1 and 30, and k varies between 1 and 512. If AP_i is perceived and AP_j is not, the corresponding field in radio map is set to +Infinity, inversely; the field is set to -Infinity. If neither AP_i nor AP_j is perceived at one RP, the corresponding field in radio map is set to 0. In the online phase, localization tests were carried out to localize target nodes at random position in front of room doors, based on RSS measurements during the normal activities in the MFB.

Results evaluation Figure 9 shows the variation of the localization mean error as a function of the number of APs varied from 6 to 14. The localization mean error decreases as the number of APs increases. The localization precision is improved when using over than 10 APs because the localization error is significantly lower. The best localization precision is equal to 1.3 m using 14 APs in the targets read range. This error can be acceptable because of the extent of the building.

Figure 10 illustrates the impact of the radio map spacing on the localization mean error. The minimum number of measurements required by CS theory was respected. Three levels of horizontal spacing of 2, 4, and 6 m were used corresponding to 512 (128×4), 256 (64×4), and 168 (42×4) RPs, respectively. As seen in Figure 10, the error and the corresponding standard deviation decrease as the radio map spacing decreases. The localization mean error decreases from 3.6 to 2.3 m when the radio map spacing drops from 6 to 4 m.

With a radio map spacing of 2 m and when the minimum number of measurements is respected, the 3D-CS based method allows determining the current right floor in most cases showing an average of localization mean error equal to 1.87 m and a standard deviation of 1.51 m. However, the 2D-CS method has higher average of localization mean error of 2.27 m and a standard deviation of 1.62 m

Because the number of target nodes is related to other parameters (the number of APs and RPs) as defined in CS theory, the maximum number of targets is limited to 8. Then, the localization precision was investigated by varying the target nodes between 2 and 8. As a result, the localization mean error seems to be insensitive to this parameter. Assume that the sparsity level, which was discussed in CS definition, is the ratio of the number of target nodes to the number of RPs. Because the sparsity levels did not exceed 5%, they cannot be significant to investigate the influence of the number of target nodes on localization mean error.

Runtime evaluation: A higher number of APs and RPs improves the localization precision but also increases the computational cost. The greater the number of target nodes results in the increase of the run time for algorithm to recover their locations. The 3D-CS method is more accurate but it is more time consuming than the 2D-CS method. The main reason of such consuming time is the tensor decomposition and HOSVD operation. However, tensor product and transposition operations take few microseconds to be executed using nowadays computers capabilities. In order to reduce the run time, parallelization of techniques, such as gradient-based, Newton and alternating least squares (ALS) methods can be used.

Comparison to prior work: Table I shows a comparison between the performance of the 3D-CS method and previous experimental work based on different localization techniques. Different comparison criterions were considered a seen in Table I. We observe that the 3D-CS method is better in terms of practicability, computational and

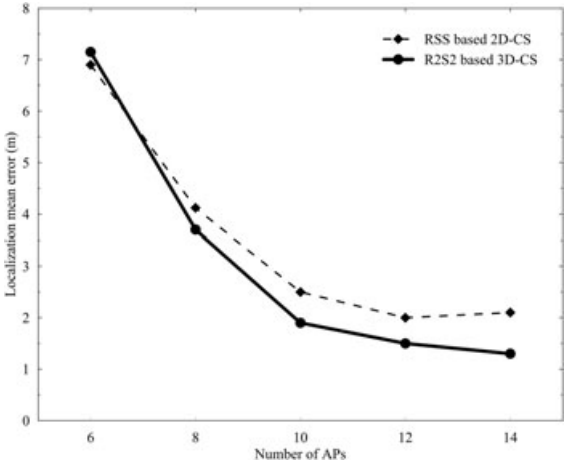

Figure 9. Influence of the number of APs on localization mean error determined by experimental results.

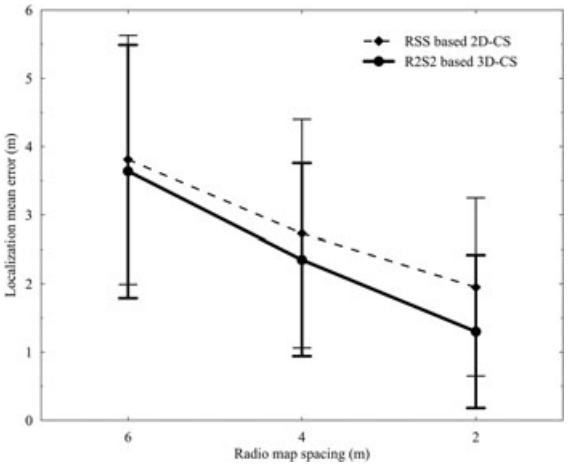

Figure 10. Influence of the radio map spacing on localization mean error determined by experimental results.

Table I. Comparison between the proposed 3D-CS method and existing localization techniques.

Criterion	**3D-CS**	**2D-CS** [31]	**Ray-tracing** [21]	**SLAM** [36]
Technique	CS	CS & Clustering	RT (6 to 8 rays)	Localization/Mapping/ Odometry
Run time	Moderate	Short	Long	Moderate
Computational cost	Low	Low	Heavy	Moderate
Monetary cost	Low	Low	High	High
Range measurement	Ratio of RSS	RSS	TOA, DOA	Laser/sonar/camera...
Sensing device	Mobile terminal	APs	Base station	Mobile terminal
Computing device	Mobile terminal	Base Station	Dedicated station	Mobile terminal
Fingerprinting	Radio map	Radio map	Reference data	Landmark
RPs spacing	2m	1.5m	$0.4m^1$ - $0.8m^2$	-
Dimensions	3D	2D	2D	2D-3D
Area	$80 \times 60 \times 16$ m	30×46 m	85×120 m	500×250 m
Localization area	Multi-floor	Single-floor	Single-floor	Single-floor
Target number	Multiple	Multiple	Single	Single
Accuracy	1.8 m - Right floor	1.5 m	$0.2828m^1$ - $0.5657m^2$	<1m

monetary cost. In addition, our method is well suitable for localization in MFB due to reliable position estimation of multiple targets in both horizontal and vertical directions.

7. CONCLUSION

In this work, a 3D-CS method using received signals dual metrics was applied for multiple target nodes localization in MFB. The proposed solution allows a reliable estimation of the horizontal position and identification of the floor number using existing wireless networks infrastructure and a radio map, which is created in offline phase. Both simulations and experiments showed that the localization precision is enhanced when the number of APs increases and the radio map spacing decreases. The results indicated that the 3D-CS method allows superior performance in NLOS condition with significant propagation medium variation than 2D-CS method. The localization precision is improved by about 0.4 m compared with 2D-CS method. The proposed method can be applied with different wireless technologies offering a good alternative to conventional techniques for environment monitoring or traffic management systems.

REFERENCES

1. Department of Defence. *Global Positioning System Standard Positioning Service Performance Standard* (4th Edition), Assistant Secretary of Defense for Command, Control, Communications, and Intelligence. Washington, 2008.
2. Hegarty CJ, Chatre E. Evolution of the Global Navigation Satellite System (GNSS). *Proceedings of the IEEE* 2008; **96**(12): 1902–1917.
3. Arnold LL, Zandbergen PA. Positional accuracy of the wide area augmentation system in consumer-grade GPS units. *Computers & Geosciences* 2011; **37**(7): 883–892.
4. Departement of Economic and Social Affairs. *World Urbanization Prospects The 2014 Revision Hoghlights*. United Nation 2014: ISBN 978-92-1-15157-6.
5. Hightower J, Borriello G. Location systems for ubiquitous computing. *IEEE Computer* 2001; **34**(8): 57–66.
6. Donoho DL. Compressed sensing. *IEEE Transactions Information Theory* 2006; **52**(4): 1289–1306.
7. Baraniuk RG. Compressive sensing. *IEEE Signal Processing Mag* 2007; **24**(4): 118–120.
8. Abid MA, Cherkaoui S. Wireless Technlogy Agnostic Real-Time Localization in Urban Areas. In *Proceedings of the 4th IEEE LCN International Workshop on Wireless and Internet Services (WISe)*, 2011.
9. Bouet M, Dos Santos AL. *RFID tags: Positioning principles and localization techniques. Wireless Days*, 2008. WD 08: 1st IFIP: 1–5.
10. Paul AS, Wan EA. Wi-Fi based indoor localization and tracking using sigma-point Kalman filtering methods. In *Position, Location and Navigation Symposium IEEE/ION*, 2008; 646–659.
11. Beucher PJ. *Asset localization identification and movement system and method. U.S. Patent*, 2011. 7 957 833 B2.
12. Varshavsky A, LaMarca A, Hightower J, de Lara E. The SkyLoc Floor Localization System. In *Pervasive Computing and Communications PerCom Fifth Annual IEEE International Conference*, 2007; 125–134.
13. Ahmad U, Dauriol BJ, Young-Koo LEE, Sungyoung LE. Multi-Floor Semantically Meaningful Localization Using IEEE 802.11 Network Beacons. *IEICE transactions on communications* 2008; 3450–3460.
14. Maroti M, Volgyesi P, Dora S, Kusy B, Nadas A, Ledeczi A, Molnar K. Radio interferometric geolocation. In *Proceedings of the 3rd International Conference on Embedded Networked Sensor Systems ACM*, 2005; 1–12.

15. Castellanos JA, Tardos JD. *Mobile robot localization and map building: A multisensor fusion approach*. Kluwer academic publishers: Norwell, MA, USA, 2000.
16. Schwarz V, Huber A, Tuchler M. Accuracy of a commercial UWB 3D location/tracking system and its impact on LT application scenarios. In *IEEE International Conference on Ultra-Wideband*, 2005; 599–603.
17. Bailey T, Durrant-Whyte H. Simultaneous localization and mapping (SLAM): part II. *Robotics & Automation Magazine, IEEE* 2006; **13**(3), DOI: 10.1109/MRA.2006.1678144.
18. Woodman O, Harle R. Pedestrian localisation for indoor environments. In *Proceedings of the 10th International Conference on Ubiquitous Computing ACM*, 2008; 114–123.
19. Hightower J, Want R, Borriello G. SpotON: An Indoor 3D Location Sensing Technology Based on RF Signal Strength. *Technical Report Technology Reports UW CSE*, University of Washington, 2000.
20. Coco S, Laudani A, Mazzurco L. A novel ray tracing procedure for the localization of EM field sources in urban environment. *IEEE Transactions Magazine* 2004; **40**(2): 1132–1135.
21. Tayebi A, Gomez J, Saez de Adana F, Gutierrez O. The application of ray-tracing to mobile localization using the direction of arrival and received signal strength in multipath indoor environments. *Progress in Electromagnetics Research* 2009; **91**: 1–15.
22. Meng J, Li H, Han Z. Sparse event detection in wireless sensor networks using compressive sensing. In *Proceedings of the 43rd Annual Conference on Information Sciences and Systems (CISS)*, 2009; 181–185.
23. Xian Q, Zhang W. Adaptive Localization Algorithm Based on Distributed Compressed Sensing in Wireless Sensor Networks. *Journal of Networks* 2014; **9**(7): 1900–1907.
24. Mostofi Y, Sen P. Compressive cooperative sensing and mapping in mobile networks. In *Proceedings Conference on American Control Conference (ACC'09)*, 2009; 3397–3404.
25. Chen S, Donoho DL, Saunders MA. Atomic decomposition by basis pursuit. *SIAM Journal Sciences Computation* 1998; **20**(1): 33–61.
26. Joel AT, Anna CG. Signal recovery from random measurements via orthogonal matching pursuit. *IEEE Transactions on Information Theory* 2007; **53**(12).
27. Lu W, Vaswani N. Modified BPDN for noisy compressive sensing with partially known support. In *Proceedings of IEEE International Conference Acoustics, Speech, Signal Process (ICASSP)*, 2010; 3926–3929.
28. Kim D, Trzasko J, Smelyanskiy M, Haider C, Dubey D, Manduca A. High-performance 3D compressive sensing MRI reconstruction using many-core architectures. *International Journal of Biomedical Imaging* 2011; **2011**: 2.
29. Quinsac C, Basarab A, Gregoire JM, Kouame D. 3D compressed sensing ultrasound imaging. In *Proceedings of IEEE International Ultrasonics Symposium (IUS)*, San Diego, USA, 2010.
30. Feng C, Valaee S, Tan ZH. Multiple target localization using compressive sensing. In *Proceedings of IEEE GLOBECOM*, 2009; 1–6.
31. Feng C, Au WSA, Valaee S, Tan Z. Received-Signal-Strength-Based Indoor Positioning Using Compressive Sensing. *IEEE Transactions on Mobile Computing* 2012; **11**(12): 1983–1993.
32. Kolda TG, Bader BW. Tensor decompositions and applications. *SIAM Review* 2009; **51**(3): 455–500.
33. Kruskal JB. Rank, decomposition, and uniqueness for 3-way and N-way arrays. In *Multiway Data Analysis*. North-Holland Publishing Co, Amsterdam, The Netherlands, 1989; 7–18.
34. Sarkar TK, Ji Z, Kim K, Medour A, Salazar-Palma M. A survey of various propagation models for mobile communication. *IEEE Antennas Propagation Magazine* 2003; **45**(3): 51–82.
35. Lott M, Forkel I. A multi-wall-and-floor model for indoor radio propagation. *Vehicular Technology Conference VTC Spring. IEEE VTS 53rd* 2001; **1**: 464–468.
36. Kummerle R, Steder B, Dornhege C, Ruhnke M, Grisetti G, Stachniss C, Alexander Kleiner A. On measuring the accuracy of SLAM algorithms. *Autonomous Robots* 2009; **27**(4): 387–407.

AUTHORS' BIOGRAPHIES

Mohamed Amine Abid is a PhD candidate at the Department of Electrical and Computer engineering at the Université de Sherbrooke, Qc, Canada. He received the MScA degree in electrical engineering from the Université de Sherbrooke. His main areas of research interest include mobile and vehicular Wireless Network, radio navigation, combinatorial optimization and Artificial intelligence.

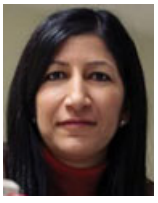

Soumaya Cherkaoui is a full professor at the Department of Electrical and Computer Engineering of Université de Sherbrooke, Canada, which she joined in 1999. She holds a bachelor's degree in Computer Engineering from EMI Engineering School (École Mohammedia

D'Ingénieurs), Rabat (Morocco) and a PhD in Electrical Engineering from Université de Sherbrooke. Since 2005, she has been the director of INTERLAB, a research laboratory that conducts research funded both by government and industry. Prior to her appointment at U.Sherbrooke, Cherkaoui worked for industry as a project leader on projects targeted at the Aerospace Industry. Cherkaoui has more than 100 publications in reputable journals, conferences, and workshops in the area of communication networks. Her research and teaching interests are in wireless ad hoc and sensor networks. She is an accredited Professional Member of the Order of Engineers of Quebec and a senior IEEE member.

Wirel. Commun. Mob. Comput. 2016; **16**:1837–1850 © 2015 John Wiley & Sons, Ltd.
DOI: 10.1002/wcm